science, engineering and health studies

Research Article

Science, Engineering and Health Studies
https://li01.tci-thaijo.org/index.php/sehs
ISSN (Online): 2630-0087

Distribution of precipitable water over Thailand using MTSAT-1R satellite data

Sumaman Buntoung[1], Serm Janjai[1], Jindarat Pariyothon[1] and Manuel Nunez[2]*

[1] Department of Physics, Faculty of Science, Silpakorn University, Nakhon Pathom 73000, Thailand
[2] Geography and Spatial Sciences Discipline, School of Science and Technology, University of Tasmania, Hobart 7001, Australia

***Corresponding author**:
Serm Janjai
serm.janjai@gmail.com

***Received**: 8 March 2020*
***Revised**: 10 October 2020*
***Accepted**: 20 October 2020*
***Published**: 30 January 2021*

***Citation**:
Buntoung, S., Janjai, S., Pariyothon, J., and Nunez, M. (2021). Distribution of precipitable water over Thailand using MTSAT-1R satellite data. Science, Engineering and Health Studies, 15, 21020001.

ABSTRACT

In this study, we investigated the long-term spatial distribution of atmospheric precipitable water vapor (PWV) in Thailand using a statistical model that relates the satellite-derived brightness temperature to the PWV. In the validation process, we used an independent dataset obtained from PWV measurements at four stations, for which the mean of the PWV is 4.42±1.06 cm and that of the model is 4.42±0.89 cm. This result indicates that the model performs well. After validation, the model was used to calculate PWV based on satellite data for the whole country at a spatial resolution of 4 km × 4 km and the results of which are presented as monthly and yearly PWV maps. The monthly PWV maps reveal that the PWV values are relatively high throughout the country during the wet season (May-October) and low in the dry season (November-April). The yearly PWV map indicates that the PWV varies with latitude, with low values in the north that gradually increase to high values in the south.

Keywords: precipitable water; brightness temperature; weather satellite; spatial distribution; seasonal distribution

1. INTRODUCTION

Water vapor is a meteorological parameter that has an important role in atmospheric chemical and physical processes. In the troposphere, water vapor influences the optical properties of aerosols, which results in clouds and rain (Kämpfer, 2013). It also has an impact on visibility (Iqbal, 1983). Moreover, water vapor can absorb atmospheric radiation and is one of the most active greenhouse gases. Water vapor is reported to contribute more than 60% of the natural greenhouse effect (Taylor, 2005). This is because atmospheric water vapor allows most ultraviolet and visible radiation to pass to the Earth's surface but absorbs a large fraction of the infrared radiation emitted by the Earth's surface (Iqbal, 1983; Nunez, 1993). Although the upper atmosphere contains very little water vapor, it can affect the circulation and stability of the atmosphere (Kämpfer, 2013). In summary, water vapor significantly influences the surface and atmospheric energy balance and detailed study of its behavior and distribution is warranted.

In general, water vapor in the atmosphere depends on a surface water source (Wang, 2013), which is influenced by agricultural activities, forests, hydrology, and the geographical landscape. For example, over a large-scale desert, the concentration of water vapor is extremely low (Basha, 2013) due to scarcity of surface water. Over seas and oceans in the tropics, the concentration of water vapor is generally high (Prabhakara et al., 1982) due to the abundance of the surface water. Water vapor also varies with the season (Gurbuz and Jin, 2017), which means the atmospheric water vapor changes with geographical regions and seasons.

In general, water vapor is measured in terms of precipitable water vapor (PWV) using ground-based instruments, e.g., the microwave radiometer, sunphotometer, and upper-air radiosonde (Cuomo et al., 1997). However, these instruments have limited general use due to their high cost. An alternative and less costly solution is to use a classical modeling approach (Reitan et al., 1960; Hay et al., 1971) to determine atmospheric PWV based on temperature and relative humidity data. The above studies depicted the amounts of PWV in contour maps of the entire country. However, this approach is complicated and requires certain input data that may not be available. Another solution is to use data retrieved from satellites to estimate the PWV at regional and global scales (Takeuchi et al., 2010). Larsen and Stamnes (2005) developed a technique for calculating the amount of water vapor in atmospheric haze based on the radiation reflected from the ground and retrieved by satellite sensors. Lee and Park (2007) conducted a study and tested a model for determining the amount of water vapor in the East Asian area based on the brightness temperature at wavelengths of 11 and 12 μm, as these wavelengths are sensitive to water vapor. These data were obtained from the GOES-9 and MTSAT-1R satellites. Using this technique, the authors retrieved PWV measurements with a satisfactory level of uncertainty and a root mean square difference of about 0.58 cm. Similarly, Akatsuka et al. (2010) used brightness temperature data from the MTSAT satellite to calculate PWV in East and Southeast Asia and the western Pacific. The model results and measured data agreed to within a root mean square difference of 11.08%. Gurbuz and Jin (2017) investigated the long-time variation of PWV estimated from the Global Positioning System (GPS), the moderate resolution imaging spectroradiometer (MODIS) onboard polar-orbiting satellites, and radiosonde observations, and found that the variations in the PWV obtained using these three techniques were in agreement. Liu et al. (2020) proposed a physics-based algorithm for retrieving PWV using satellite passive microwave observations and also obtained satisfactory results.

Thailand, located in the tropics, exhibits large seasonal changes in PWV that warrant closer examination. In addition, the investigation of PWV in Thailand has been very limited (Exell, 1978; Phokate and Atyotha, 2018; Charoenphon and Satirapod, 2020). To the best of our knowledge, the long-term behavior of PWV over Thailand has not been reported. In this study, we investigated the long-term behavior of atmospheric PWV distributions over Thailand. Although 12-hour and daily PWV maps are available (http://wxmaps.org/fcst.php) for the entire globe, which are produced by the Center for Ocean-Land-Atmosphere Studies (COLA) of George Mason University, these maps depict only the short-term behavior of PWV and could not be used for this study.

To formulate an empirical model for this study, we used satellite data in the water vapor channel that is sensitive to atmospheric water. After validating this model against an independent dataset, we used it to estimate PWV over Thailand based on 9-year satellite data. The results are represented as long-term PWV maps, on both monthly and yearly bases.

2. MATERIALS AND METHODS

To estimate PWV from meteorological satellite data obtained over Thailand, we used concurrent satellite brightness temperature data in the infrared wavelength and ground-based measured PWV data.

2.1 Materials

The materials used in this research included satellite- and ground-based data, the details of which are described in the following.

2.1.1 Satellite data

We used data obtained by the Japanese geosynchronous weather satellite MTSAT-1R, which covers East and Southeast Asia and the western Pacific region. This satellite captures hourly image data on five channels, including one channel in the visible wavelength, two channels in the thermal infrared wavelengths, one channel in the near-infrared wavelength, and a water vapor channel (Takeuchi et al., 2010). To examine PWV variability in the Thailand region, we used nine years (2007-2015) of data from the water vapor channel (6.2-7.3 μm), which have a spatial resolution of 4 km × 4 km.

Using a computer program written in Interactive Data Language, the satellite data were sectorized for the entire Thailand area (Figure 1A). The satellite map projection data were then converted to cylindrical projection and the images were navigated using several coastlines as references. Each satellite image covers latitudes 4.9°N-20.8°N and longitudes 96.0°E-106.0°E, and consists of 550 × 850 pixels (Figure 1B). Each pixel contains a gray-level value as digital 10-bit data (0 to 1023) (Janjai et al., 2011). The gray level of each satellite pixel was converted to a relevant atmospheric parameter, e.g., brightness temperature (T_B), using a conversion table provided by the satellite agency (Figure 2) (https://www.data.jma.go.jp/mscweb/en/operation/mt1r_hrit.html).

These data were obtained on an hourly basis from January 2007 to December 2015 and were then processed to obtain a monthly average. The monthly brightness temperature data were used for modeling and validation, and for mapping the PWV.

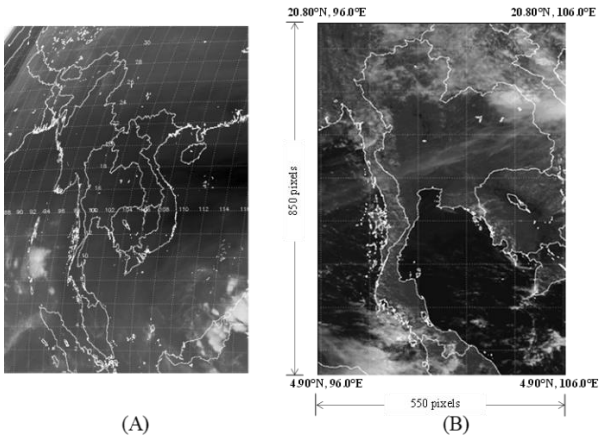

Figure 1. Satellite images in (A) satellite projection and (B) cylindrical projection

2.1.2 Ground-based data

PWV values measured by sunphotometers (CE-318) were used to create a model for calculating PWV and testing the performance of the model. The sunphotometer measures the surface direct spectral irradiance, and has nine channels: 340, 380, 440, 500, 675, 870, 937, 1020,

and 1640 nm. To determine amounts of water vapor, the data obtained in the 937-nm wavelength are used (Halthore et al., 1997). These instruments were installed at the four main meteorological stations in Thailand, i.e., Chiang Mai (18.98°N, 98.98°E), Ubon Ratchathani (15.25°N, 104.87°E), Nakhon Pathom (13.82°N, 100.04°E) and Songkhla (7.20°N, 100.60°E) (Figure 3). The sunphotometers, which are owned by the Tropical Atmospheric Physics Laboratory of Silpakorn University, are also part of the Aerosol Robotic Network (AERONET) organized by NASA. The AERONET processes raw data obtained by these sunphotometers and makes these processed data freely available on the Internet. For this study, we downloaded the PWV data obtained by these instruments during the 2007-2015 period from the AERONET website at https:// aeronet.gsfc. nasa.gov, which we then processed into monthly average PWV data.

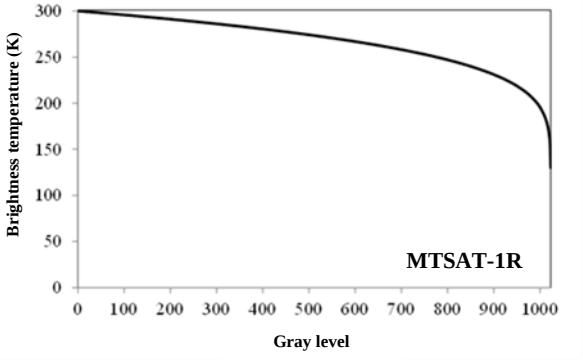

Figure 2. Relationship between the gray level and the brightness temperature from the water vapor channel of the MTSAT-1R satellite (https://www.data.jma.go.jp/mscweb /en/operation/mt1r_hrit.html)

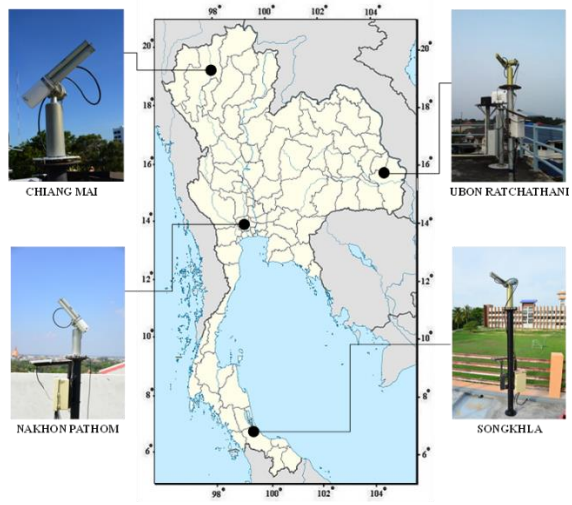

Figure 3. Locations of the four stations and photos of the sunphotometer installed at each station

2.2 Methods

The methods used in this study included modeling, model validation, and mapping. For the modeling, we collected the monthly brightness temperature data obtained by the MTSAT-1R satellite at the four stations from January 2007 to December 2013, which were then normalized with respect to the highest value (252.58 K) to obtain normalized brightness temperatures (T_B'). Similarly, the PWV data obtained from ground-based measurements were normalized with the highest value (5.47 cm) to obtain the normalized PWV (PWV′). Then, the relation between T_B' and PWV′ was determined. Normalization was performed to ensure that the two quantities had the same order of magnitude (0-1), thus reducing the uncertainty of the correlation. Next, the empirical model obtained from the correlation was used to estimate the monthly PWV, which was validated against the independent PWV data obtained at the four stations during 2014-2015. As the brightness temperature is in the form of a grid (4 km × 4 km) and the PWV is in point form, the correlation between the two quantities can generate significant error in short-term modeling. However, in this study, the two quantities were long-term averages for which with the short-term noise (random error) had been cancelled (Masiri et al., 2008; Hakuba et al., 2013). Therefore, the model in this study was expected to be sufficiently accurate for the purposes of this study, and this expectation was confirmed by validation of the model against the independent dataset.

Thailand is divided into four main geographic regions (northern, northeastern, central, and southern regions), but to avoid regional boundary problems in the application of the model, an empirical model for each region was not constructed. A model for each season was also not created because doing so would require high and low values for the input variable, which cannot be easily obtained for each season. After validation, the empirical model obtained from the correlation was used to estimate the long-term PWV behavior based on the nine years (2007-2015) of MTSAT-1R data over Thailand.

3. RESULTS AND DISCUSSION

Figure 4 shows the modeled relationship between the normalized monthly PWV obtained by the sunphotometers and the normalized monthly brightness temperature from MTSAT-1R.

The scattering of data points in Figure 4 may be due to a number of factors, such as the failure to consider other independent variables in the model that influence PWV. This issue must be investigated in future work.

The best fit obtained using the least-squares technique (Wolberg, 2006) can be expressed as a quadratic equation:

$$PWV' = a_1 + a_2 T_B' + a_3 T_B'^2, \quad (1)$$

where PWV′ is the normalized monthly PWV, T_B' is the normalized monthly T_B, and a_1, a_2, and a_3 are regression coefficients. Table 1 lists the coefficient and associated statistical values.

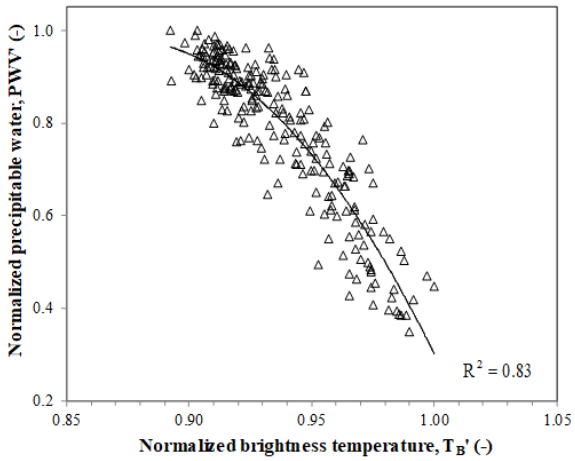

Figure 4. Relation between the normalized monthly precipitable water vapor (PWV′) obtained from the sunphotometers and the normalized monthly brightness temperature (T_B′) from the MTSAT-1R

As shown in Table 1, the t-statistic values show that the regression coefficients for all variables were significant at the 95% confidence level. Therefore, the proposed model was used to estimate the monthly PWV and the results were compared with the independent PWV data measured at the four stations. Figure 5 shows the validation results.

The difference between these datasets is presented in terms of root mean square difference (RMSD) and mean bias difference (MBD), which are expressed as follows:

$$\text{RMSD}\ (\%) = \frac{\sqrt{\frac{\sum_{i=1}^{N}(\text{PWV}_{i,\text{mod}}-\text{PWV}_{i,\text{meas}})^2}{N}}}{\frac{\sum_{i=1}^{N}\text{PWV}_{i,\text{meas}}}{N}}, \quad (2)$$

$$\text{MBD}\ (\%) = \frac{\sum_{i=1}^{N}(\text{PWV}_{i,\text{mod}}-\text{PWV}_{i,\text{meas}})}{\sum_{i=1}^{N}\text{PWV}_{i,\text{meas}}} \times 100, \quad (3)$$

where $\text{PWV}_{i,\text{mod}}$ is the PWV from the empirical model, $\text{PWV}_{i,\text{meas}}$ is the PWV measured by the ground-based sunphotometer, i is the order of the data (i = 1, 2, …, N), and N is total number of the data.

Table 1. Coefficient values and related statistic values.

Coefficient	Value of coefficient	t-statistic	p-value	R^2	N
a_1	−31.339	−4.8186	<0.05		
a_2	73.960	5.3587	<0.05	0.83	232
a_3	−42.328	−5.7822	<0.05		

Note: R^2 is coefficient of determination and N is number of data

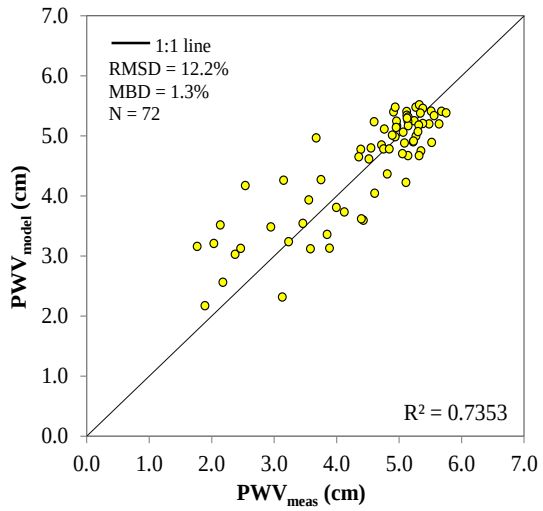

Figure 5. Comparison of the monthly PWV values calculated by the empirical model (PWV_{model}) with those measured by the ground-based sunphotometers (PWV_{meas}) at the four stations in Thailand

The results in Figure 5 show that, when compared with the ground-based measured data, this model determined PWV values with an RMSD of 12.2% and an MBD of 1.3%. It could be seen that the data points in Figure 5 are more scattered for the low values of PWV and less so for high PWV values, which can be explained as follows. The scatter points correspond with the dry season, during which the predominant atmospheric condition is clear skies. In these conditions, there is greater interference from the ground to the satellite signal, which causes more errors in the satellite-derived brightness temperature. In contrast, for high values of PWV, which usually occur in the wet season, the skies are frequently covered by cloud, which cause less interference from the ground to the satellite signal, which results in fewer errors in the satellite-derived brightness temperature than in the dry season. However, overall, this result can be considered to be acceptable in this field (Wong, 2015). Therefore, the model can be reliably used to calculate water vapor over Thailand.

After validation, PWV values were calculated by the empirical model for the nine-year period (2007-2015). The results in terms of monthly and yearly PWV maps are shown in Figures 6 and 7, respectively. Figure 6 shows the distribution of monthly PWV over Thailand, in which we can clearly see that the PWV in this region varies strongly at temporal and spatial scales. These variations are due to the influence of local monsoons. From November to February, which is the period of northeast monsoon, there is less water vapor in the atmosphere in the northern and central parts of the country as dry air is transported from China. In the southern part, there is more PWV because the monsoon brings rain to this region. The March-April period is a calm period with high ambient air temperatures that result in increases in the PWV. For the period of May to October, the country is influenced by the southwest monsoon, which transports moist air from the Andaman Sea into Thailand and results in a high PWV values. This result is consistent with the distribution of rainfall in Thailand (Janjai et al., 2015). In terms of geographical distribution (Figure 7), PWV gradually increases from the north to the south of the country, with the south having relatively high PWV values, as compared with other parts of the country. This result agrees with the study by Charoenphon and Satirapod (2020), in which a GPS approach was used.

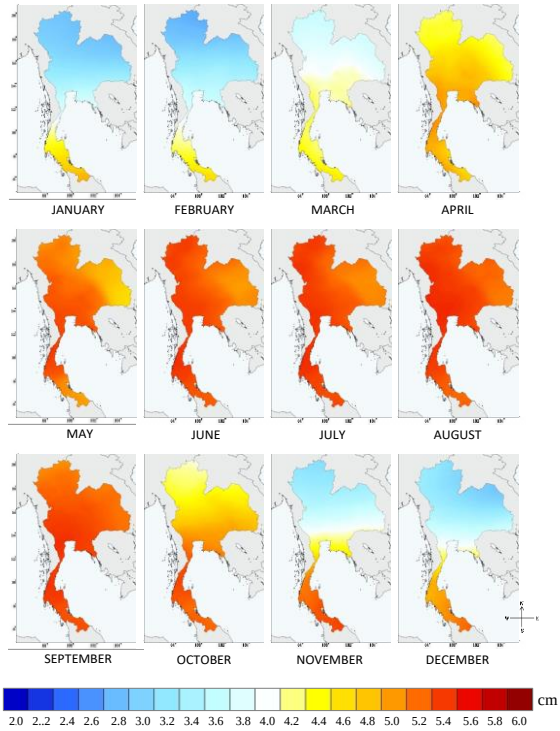

Figure 6. Monthly average precipitable water over Thailand

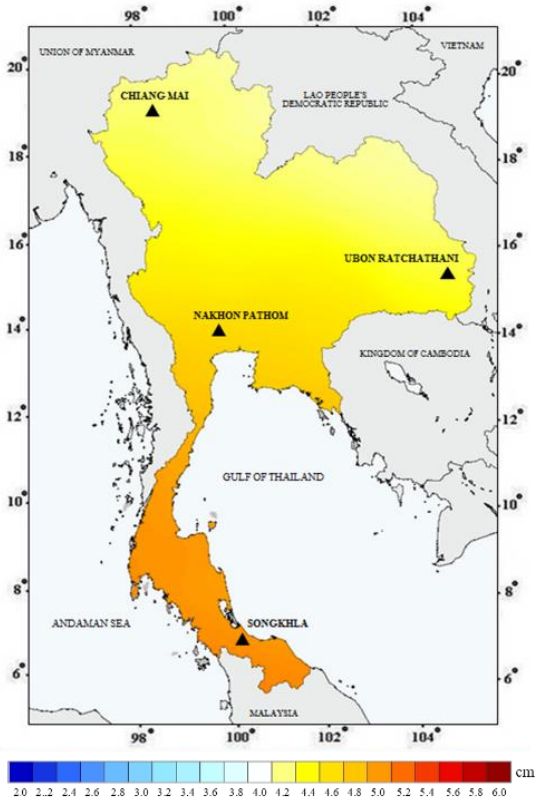

Figure 7. Yearly average precipitable water over Thailand

4. CONCLUSION

In this study, the long-term spatial distribution of PWV over Thailand was examined using a model relating satellite-derived brightness temperature and ground-based measurements of PWV, with the results displayed as monthly and yearly PWV maps. PWV value was found to be relatively high over the country in the wet season (May-October) and low in the dry season (November-April). The yearly PWV map shows that PWV varies with latitude, with low values in the north and high values in the south of the country. In addition, the variation in the yearly PWV from the north to the south ranges from 4.15 to 5.07 cm. These results indicate that PWV may significantly affect the weather and climate of different parts of the country. As there might be other factors influencing PWV, we recommend the investigation of these factors in future work.

ACKNOWLEDGMENT

The authors would like to thank the Thailand Research Fund (TRF, RDG59300001) for its financial support of this research. We are also grateful to the Thai Meteorological Department for its permission to install sunphotometers at its regional meteorological stations. AERONET of NASA is gratefully acknowledged for providing PWV data.

REFERENCES

Akatsuka, S., Oyoshi, K., and Takeuchi, W. (2010). Mapping of precipitable water using MTSAT data. In *Proceedings of 31st Asian Conference on Remote Sensing (ACRS)*, pp. 1584-1589. Hanoi, Vietnam.

Basha, S. G. (2013). *Studies on Vertical Distribution of Atmospheric Water Vapor: Atmospheric Water Vapor*, Germany: Lambert Academic Publishing, pp. 1-39.

Charoenphon, C., and Satirapod, C. (2020). Improving the accuracy of real-time precipitable water vapour using country-wide meteorological model with precise point positioning in Thailand. *Journal of Spatial Science*, 2020, 1-17.

Cuomo, V., Tramutoli, V., Pergola, N., Pietrapertosa, C., and Romano, F. (1997). In place merging of satellite based atmospheric water vapour measurements. *International Journal of Remote Sensing*, 18(17), 3649-3668.

Exell, R. H. B. (1978). The water content and turbidity of the atmosphere in Thailand. *Solar Energy*, 20(5), 429-430.

Gurbuz, G., and Gin, S. (2017). Long-time variations of precipitable water vapour estimated from GPS, MODIS and radiosonde observations in Turkey. *International Journal of Climatology*, 37(15), 5170-5180.

Hakuba, M. Z., Folini, D., Sanchez-Lorenzo, A., and Wild, M. (2013). Spatial representativeness of ground-based solar radiation measurements. *Journal of Geophysical Research: Atmosphere*, 118(15), 8585-8597.

Halthore, R. N., Eck, T. F., Holben, B. N., and Markham, B. L. (1997). Sun photometric measurements of atmospheric water vapor column abundance in the 940-nm band. *Journal of Geophysical Research: Atmospheres,* 102(D4), 4343-4352.

Hay, J. E. (1971). Precipitable water over Canada: II Distribution. *Atmosphere*, 9(4), 101-111.

Iqbal, M. (1983). *An Introduction to Solar Radiation*. New York: Academic Press, pp. 128-133.

Janjai, S., Masiri, I., Pattarapanitchai, S., and Laksanaboonsong, J. (2011). An improved model for the estimation of solar radiation from satellite data for Thailand. *Journal of the Institute of Engineering*, 8(3), 130-139.

Janjai, S., Nimnuan, P., Nunez, M., Buntoung, S., and Cao, J. (2015). An assessment of three satellite-based precipitation data sets as applied to the Thailand region. *Physical Geography*, 36(4), 282-304.

Kämpfer, N. (2013). Introduction. In *Monitoring Atmospheric Water Vapour* (Kämpfer N., eds.). pp. 1-7. New York: Springer.

Larsen, N. F., and Stamnes, K. (2005). Use of shadows to retrieve water vapor in hazy atmospheres. *Applied Optics*, 44(32), 6986-6994.

Lee, K. M., and Park, J. H. (2007). Retrieval of total precipitable water from the split-window technique in the East Asian region. In *Proceedings of the EUMETSAT Meteorological Satellite Conference*, pp. 1-8. Amsterdam, Netherlands.

Liu, H., Li, H., Tang, S., Duan, M., Zhang, S., Deng, X., and Hu, J. (2020). A physical algorithm for precipitable water vapour retrieval over land using passing microwave observations. *International Journal of Remote Sensing*, 41(16), 6288-6306.

Masiri, I., Nunez, M., and Weller, E. (2008). A 10-year climatology of solar radiation for the Great Barrier Reef: implications for recent mass coral bleaching events. *International Journal of Remote Sensing*, 29(15), 4443-4462.

Nunez, M. (1993). The development of a satellite-based insolation model for the tropical western Pacific Ocean. *International Journal of Climatology*, 13(6), 607-627.

Phokate, S., and Atyotha, V. (2018). Determination of the amount of water vapor in the troposphere over Thailand using surface data. *Kasem Bundit Engineering Journal*, 8, 364-372.

Prabhakara, C., Chang, H. D., and Chang, A. T. (1982). Remote sensing of precipitable water over the oceans from Nimbus 7 microwave measurements. *Journal of Applied Meteorology and Climatology*, 21(1), 59-68.

Reitan, C. H. (1960). Distribution of precipitable water vapor over the Continental United States. *Bulletin of the American Meteorological Society*, 41(2), 79-87.

Takeuchi, W., Nemoto, T., Kaneko, T., and Yasuoka, Y. (2010). Development of MTSAT data processing, distribution and visualization system on WWW. *Asian Journal of Geoinformatics*, 10(3), 29-33.

Taylor, F. W. (2005). *Elementary Climate Physics*. Oxford: Oxford University Press, pp. 104-118.

Wang, P. K. (2013). *Physics and Dynamics of Clouds and Precipitation*. Cambridge: Cambridge University Press, pp. 1-26.

Wolberg, J. (2006). *Data Analysis Using the Method of Least Squares: Extracting the Most Information from Experiments*. Berlin: Springer, pp. 31-71.

Wong, M. S., Jin, X., Liu, Z., Nichol, J. E., Ye, S., Jiang, P., and Chan, P.W. (2015). Geostationary satellite observation of precipitable water vapor using an empirical orthogonal function (EOF) based reconstruction technique over eastern China. *Remote Sensing*, 7(5), 5879-5900.